Bachelor Thesis

Measurement of PMT dark rates for the IceCube mDOM

submitted to obtain the academic degree Bachelor of Science

Presented by

Anna Eimer

04 May 2021

Erlangen Centre for Astroparticle Physics
Friedrich-Alexander University Erlangen-Nürnberg

Supervisors: Prof. Dr. Uli Katz

Abstract

The IceCube Neutrino Observatory at the South Pole is a Cherenkov detector built to discover astrophysical high-energy neutrino emission, to search for dark matter and many other things. The IceCube Upgrade is currently being built and will, amongst others, consist of multi-PMT digital optical modules, called mDOMs.

The neutrino-induced Cherenkov light is measured by Photomultiplier tubes (PMTs) contained in a pressure resistent glass vessel. An important property of the PMTs is the dark rate, especially at low temperatures, since the mDOMs are operated in the Antarctic ice.

In this Thesis the dark rate of the PMT model used for the mDOM will be measured in three different ways at different temperatures. These different methods will be compared.

Zusammenfassung

Das IceCube Neutrino Observatorium am Südpol ist ein Cherenkov-Detektor zur Erforschung astrophysikalischer, hochenergetischer Neutrino Emission, Dunkler Materie und vielem mehr. Die IceCube Erweiterung, die momentan gebaut wird, besteht unter anderem aus Multi-PMT digitalen optischen Modulen, sogenannten mDOMs.

Das Neutrino-induzierte Cherenkov-Licht wird mit Photomultiplier-Röhren (PMTs) gemessen, die sich in einem druckfesten Glasgefäß befinden. Eine wichtige Eigenschaft der PMTs ist die Dunkelrate, insbesondere bei tiefen Temperaturen, da die mDOMs im antarktischen Eis betrieben werden.

In dieser Arbeit wird die Dunkelrate des PMT-Modells, das für das mDOM genutzt wird, auf drei verschiedene Arten bei verschiedenen Temperaturen gemessen. Diese Methoden werden verglichen.

Contents

1 Introduction **7**
- 1.1 Motivation . . . 7
- 1.2 IceCube . . . 7
- 1.3 Photomultiplier Tubes . . . 9
  - 1.3.1 Working principle . . . 10
  - 1.3.2 Single photoelectron spectrum . . . 12
  - 1.3.3 Correlated pulsed background . . . 14
  - 1.3.4 Dark rate . . . 15

2 Experimental setup **17**

3 Explanation of the different measurement methods **21**
- 3.1 Method 1 . . . 21
- 3.2 Method 2 . . . 22
- 3.3 Method 3 . . . 22
- 3.4 Measurements with light source . . . 24

4 Measurements **27**
- 4.1 Gain Measurements . . . 27
- 4.2 Threshold Measurements . . . 28
- 4.3 Temperature Measurements . . . 31

5 Analysis and Comparison of the methods **37**

6 Conclusion **39**

1 Introduction

This chapter motivates the thesis and introduces the IceCube project. Furthermore, the functionality and the dark rate behaviour of photomultiplier tubes will be discussed.

1.1 Motivation

The main goal of this thesis is to compare different methods to measure the dark rate of photomultiplier tubes for the IceCube mDOM. Therefore three approaches will be used to ideally produce the same results.

So far Münster and Erlangen used two different procedures for the dark rate measurement and got different results, which should not be the case. This thesis should help to solve this confusion. The third method is used as additional opportunity for comparison.

1.2 IceCube

The IceCube observatory is a Cherenkov detector located at the South Pole. The main goals of the experiment are the discovery of Galactic and extragalactic sources of high-energy neutrino emission. It is also suited for the search for dark matter, cosmic ray investigations and neutrino oscillation measurements.[1]

The submerged "In-Ice" detector consists of 86 strings each equipped with 60 digital optical modules (DOMs). Each DOM is autonomously operating a 25 cm photomultiplier tube (PMT) in a glass pressure housing, currently deployed at depths between 1450 m and 2450 m (see figure 1.1, blue). The glacial ice behaves as interaction medium and support structure for the IceCube array. Cherenkov radiation emitted by secondary charged particles like muons or electrons produced in neutrino interactions in or near the active detector volume carries the information of the neutrino's energy, direction, arrival time and flavour. Digitized waveforms from each DOM provide the record of the event signatures in IceCube, including the arrival time and amplitude (charge) of the detected Cherenkov photons emitted by the charged particles as they traverse the ice.[1][2]

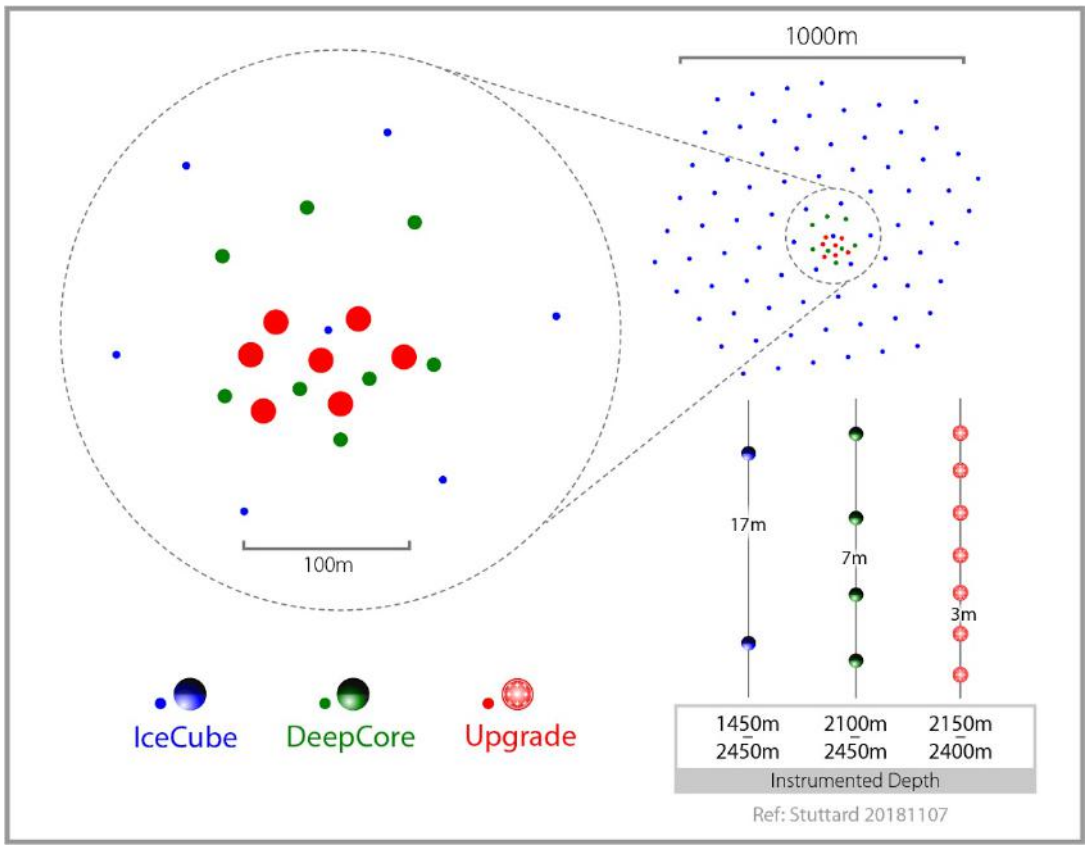

Figure 1.1: *A bird eye geometry view of the IceCube detector strings. IceCube, in blue, and the infill subdetector DeepCore, in green, show the current configuration. The red volume shows the Upgrade.[3]*

The IceCube Upgrade (figure 1.1, red) will consist of nearly 800 new optical modules attached to 7 vertical strings. New optical modules are being developed, which are expected to significantly increase the detector sensitivity. One of such concepts is the multi-PMT Digital Optical Module (mDOM) which features 24 three-inch PMTs inside a near-spherical pressure vessel resulting in a homogeneous directional sensitivity. These PMTs are pointing uniformly in all directions, providing an almost homogeneous angular coverage.[4][5] The design of such a mDOM can be seen in figure 1.2. The IceCube Upgrade will increase the precision of neutrino measurements and gives the opportunity to test the newly developed equipment for the next generation detector.

Figure 1.2: *Photograph of the IceCube Upgrade mDOM design.[6]*

In the future a next generation neutrino telescope, IceCube-Gen2, is planned to address the two main limiting factors in the current IceCube instrument: event rate and angular resolution. Furthermore, an ultra-high-energy radio array is planned to be added to expand the energy range of cosmic neutrinos by several orders of magnitude. To fully explore higher energies, where fluxes are lower, increasing the effective area of the detector array is required. The Gen2 will enclose the current detector with about 120 additional strings each equipped with up to 80 optical modules.[2]

1.3 Photomultiplier Tubes

A photomultiplier tube (PMT) is an optical sensor, often used to register fast light signals in the visible or ultraviolet regime.[7] PMTs cover a dynamic range of signals from single photons up to several thousand simultaneously arriving photons. The operation method is based on the conversion of photons to electrons via photoeffect and the multiplication of these electrons. The output signal is a charge or voltage signal, which can be measured with dedicated electronics, or as done in this thesis, with an oscilloscope.[4]

1.3.1 Working principle

The schematic of a PMT is shown in figure 1.3. It consists of an entrance window, a photocathode, focusing electrodes, an electron multiplier (so called dynodes) and an anode, usually sealed into an evacuated glass tube.

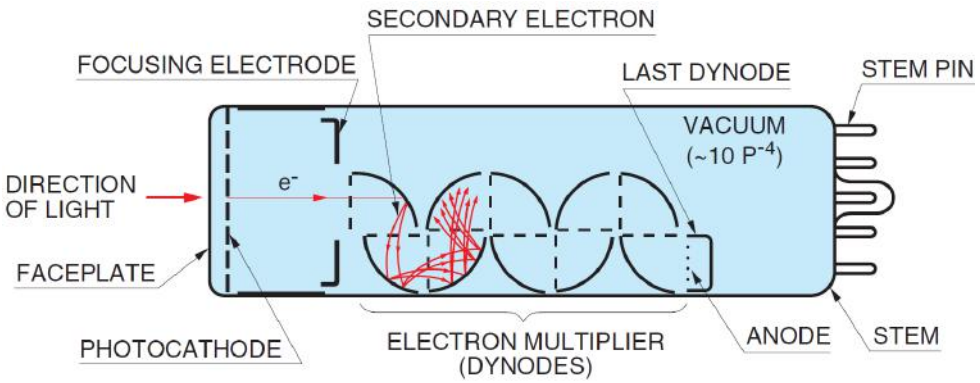

Figure 1.3: *Composition of a photomultiplier tube, consisting of an entrance window (faceplate), a photocathode, focusing electrodes, an electron multiplier and an anode.[8]*

When a photon passes through the entrance window, it can excite an electron inside the photocathode. This so-called photoelectron diffuses to the surface. In case its energy is large enough to overcome the potential barrier, the photoelectron is emitted into the vacuum (figure 1.4). This photoelectric conversion is called the external photoeffect.[8][4]

It can be also described using band models, since the photocathode is or can be described as a semiconductor (either alkali metals (shown in figure 1.5) or doped crystalline semiconductors). In the band model, a semiconductor is described by a band gap E_g that cannot be occupied by electrons, an electron affinity E_a and a work function W_{th}. The interval between conduction band and the vacuum level is called E_a. The energy difference between Fermi level and vacuum level is called W_{th}. When a photon strikes the photocathode, an electron in the valence band absorbs photon energy and is excited. If this energy is greater than the sum of E_a and E_g, a photoelectron will be emitted into vacuum.[8][4]

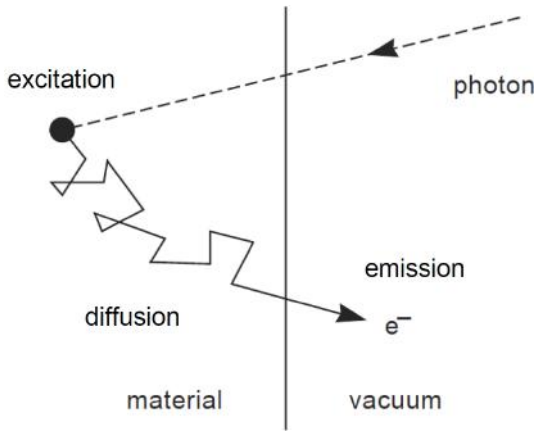

Figure 1.4: *External photoeffect. The overall process is divided in excitation, diffusion and emission.[4]*

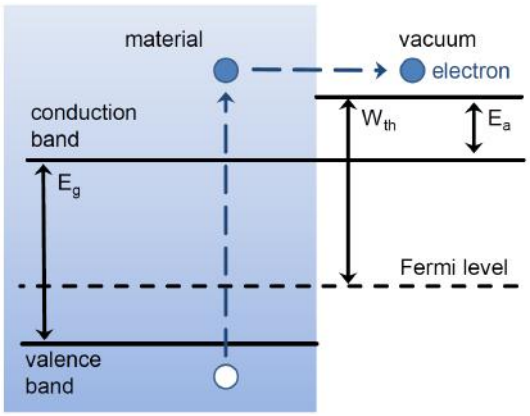

Figure 1.5: *Band model of an alkali photocathode, with band gap E_g, electron affinity E_a and work function W_{th}.[4]*

Then the photoelectron gets accelerated by the focusing electrode which directs the photoelectron to the first dynode. When the photoelectron reaches the first dynode, it produces secondary electrons. Photoelectrons are multiplied with amplifications ranging from 4 to 7 times. This is repeated at each dynode in the electron multiplier and the signal gets converted from a single electron signal into a measurable voltage pulse. An electric field, produced by voltages applied between the dynodes, guides the electrons to the subsequent dynode, accelerating them along the way.[8][4] This guidance and acceleration is done using a voltage divider. In the case of this thesis a passive base (figure 1.6) is used, meaning it does not consist of active components. It divides the output of a single high voltage power supply by using resistors and capacitors. In contrast to that, a fully operational mDOM uses active bases which produce the high voltage directly on the base.

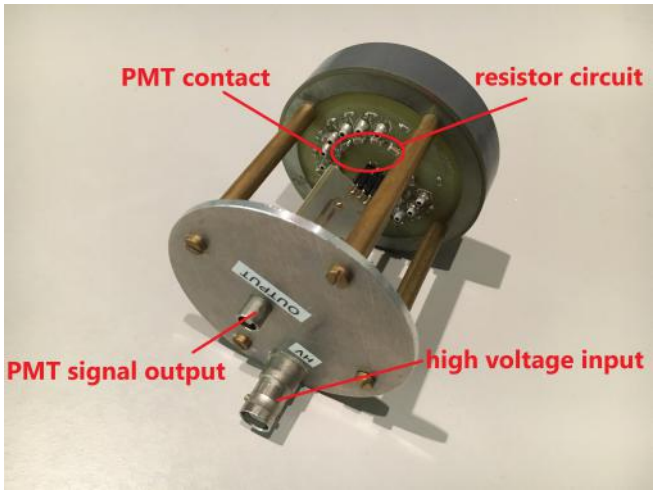

Figure 1.6: *Photograph of the passive base and its resistor circuit used in this thesis.*

When a primary electron with initial energy E_p strikes the surface of the dynode, δ secondary electrons are emitted. This number of secondary electrons per primary electron is called the secondary emission ratio δ. Using δ, the electron multiplication or gain G is expressed as follows:

$$G = \delta^n \tag{1.1}$$

where δ is the secondary emission ratio at each dynode and n is the number of dynode stages.[8]

When this cluster of electrons is finally collected at the anode, it has been multiplied by the dynodes by a factor of typically 5×10^6. The current anode signal, consisting of these electrons is either measured by dedicated electronics e.g. in the mDOM or in case of measurements in this thesis by an oscilloscope.

Another important quantity of a PMT is the quantum efficiency. It describes the probability that an incoming photon produces a photoelectron which is emitted into the vacuum.

1.3.2 Single photoelectron spectrum

The single photoelectron (abbreviated "phe") spectrum is a charge spectrum which can be acquired by integrating several output voltage waveforms as response to illumination with a pulsed light source. The principle is illustrated in figure 1.7. On the output waveform of the oscilloscope, a charge integration window (marked grey on the left part of figure 1.7) is set to a fixed width and positioned in time relative to the external trigger of the pulsed light source. In order to get a single photoelectron spectrum,

the light source is operated at a very low light output level of on average less than one photoelectron per pulse. With the light emission being a Poisson random process, the mean number of photoelectrons per pulse has to be much lower than one, for example 0.1, to reduce contamination by multi-photon events. The single photoelectron spectrum can be used to derive PMT properties like gain.[4]

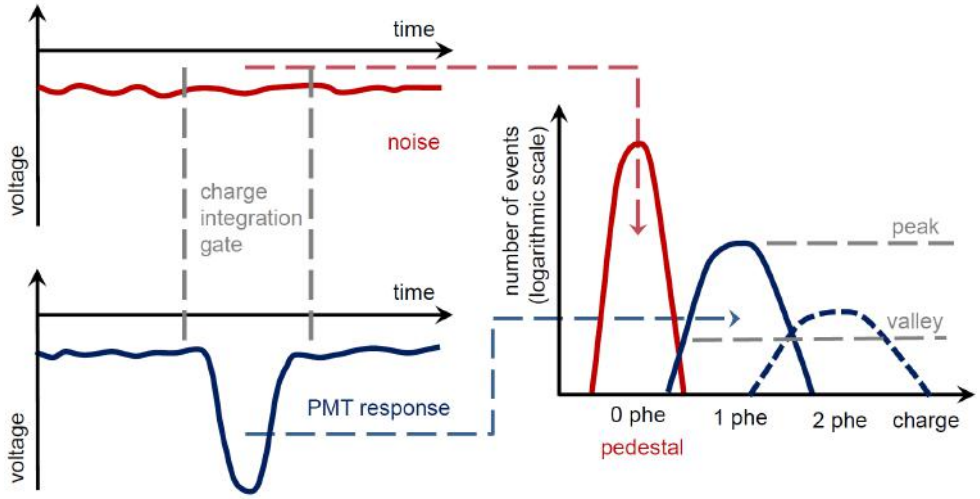

Figure 1.7: *On the left-hand side: Principle of charge spectrum acquisition from waveforms at low illumination level by a pulsed light source. Upper graph shows no signal, the lower graph shows a single photoelectron response. The area enclosed by the integration gate represents the deposited charge used to form the charge spectrum. On the right-hand side: qualitative single photoelectron spectrum splitted into its single components.[4]*

In the right part of figure 1.7, a qualitative sketch of the single photoelectron spectrum is shown. The most prominent peak (red) originates from the integration of the baseline (upper graph on the left side of figure 1.7) and corresponds to the case of zero detected photoelectrons. Its position marked by "0 phe" and "pedestal", provides a natural origin for the charge axis. The width of this peak is due to random noise. If measured with an oscilloscope, the pedestal position reflects the baseline shift relative to the true origin of the voltage axis.[4]

The blue peak with a charge of "1 phe" contains integrated single photoelectron pulses, whereas the dashed blue curve represents contamination by events with two photoelectrons. This corresponds to the lower graph on the left side of figure 1.7. The widths of the photoelectron peaks are representations of gain variations of the electron multiplier system and provides a measure for the single photon resolution.[4]

The gain can be derived from the presented distribution as

$$G = \frac{Q_{1\text{phe}} - Q_{0\text{phe}}}{e} = \frac{Q_1}{e} \tag{1.2}$$

where $Q_{0\text{phe}}$ and $Q_{1\text{phe}}$ are the respective mean charge positions of the pedestal and single photoelectron peak, Q_1 is the mean charge deposited at the anode by single photoelectron events and e is the elementary charge.[4]

1.3.3 Correlated pulsed background

Every PMT pulse can be succeeded by afterpulses or its timing characteristics can be changed resulting into early or delayed pulses. This correlated background limits signal timing and photon counting performance.[4] It also has an effect on the dark rate.

Early pulses occur if a photon crosses the photocathode without evoking an electron but producing an electron at the first dynode. This results into small pulses (lacking the amplification of the first dynode) arriving at the anode earlier than the mean transit time. The mean transit time is the time between production of the photoelectron and the arrival of the signal at the anode.[4]

Late pulses are produced by photoelectrons back-scattered from the first dynode without production of secondaries. These electrons get re-accelerated towards the first dynode by the electric field. If secondary electrons are produced the second time they hit the first dynode, the resulting pulse is delayed.[4]

There are two types of afterpulses: one type produces pulses with a short delay (several ns to several tens of ns) after the signal occurs and the other type appears with a longer delay ranging from several hundreds of ns to several µs.[8]

Most afterpulses with a short delay are caused by electrons elasticly scattering on the first dynode. Usually, the time delay of this type of afterpulses is hidden by the time constant of the subsequent signal processing circuit.[8]

Afterpulses with a longer delay are caused by the positive ions which are generated by the ionisation of residual gases in the photomultiplier tube. This kind of afterpulses is also taken into account for being a part of the dark rate. The interior of a photomultiplier tube is kept at a vacuum as high as 10^{-6} to 10^{-5} Pa, but still there exist residual gases. The molecules of the residual gases may be ionised by collisions with electrons. These positive ions return to the photocathode (ion feedback) and can produce many photoelectrons which result in afterpulses. The amplitude of this type of afterpulses depends on the type of ions (e.g. helium) and the position where they are generated.[8]

1.3.4 Dark rate

A small amount of current is produced in a photomultiplier tube even when operated in a completely dark environment. This output current is called dark current, in pulse mode, it is called dark rate. In pulse mode the PMT output is first applied to a resistor, e.g. an input resistor of an oscilloscope, and the resulting voltage pulse is measured. Ideally, the dark rate should be kept as small as possible. The dark current increases nonlinear with higher supply voltages.[8][4]

When the PMT is switched off and exposed to room illumination for a certain time and then operated in the dark again, the dark rate will increase compared to the dark rate the PMT showed before the light exposure. If the PMT has been stored in the dark for several hours after the light exposure, the dark rate will not increase.[8]

There are several components contributing to the dark rate:

Thermionic emission Since the photocathode and dynode surfaces are composed of materials with a very low work function, they emit thermionic electrons even at room temperature. This has been studied by W. Richardson, and can be described with the following equation:

$$I = A \cdot T^{5/4} e^{\frac{-e \cdot W_{th}}{k_B T}} \tag{1.3}$$

where A is a constant, T is the absolute temperature in K, e is the electron charge, W_{th} is the work function and k_B is the Boltzmann constant. This formula shows that the magnitude of the work function or the photocathode material dominates the amount of thermionic emission. It also states that the dark current decreases with decreasing temperature.[8] Since the operating temperature of the PMTs in IceCube ranges from roughly $-40\,°\mathrm{C}$ to $-10\,°\mathrm{C}$, the contribution of thermionic emission to the overall dark rate is reduced compared to PMTs operating e.g. at room temperature.[8]

Leakage current (ohmic leakage) Photomultiplier tubes are operated at high voltages from 500 up to 3000 V (in this case up to 1400 V), but they also handle very low currents in the microampere range. Therefore, the quality of the insulating materials used in the tubes is very important. The relationship between the leakage current from the insulating materials and the supply voltage is determined by Ohm's law:

$$I = \frac{V}{R} \tag{1.4}$$

where I represents the current value, V the supply voltage and R is the insulation resistance. The gain has no effect on the leakage current. The dark current resulting from thermionic emission varies exponentially with the supply voltage, thus the leakage current has a larger effect on the dark current as the supply voltage is lowered.[8]

Scintillation from the glass envelope or electrode support materials Some electrons emitted from the photocathode or dynodes can deviate from their normal trajectories and do not contribute to the output signal. If these stray electrons impinge on the glass envelope, scintillations may occur and result into additional pulses which add to the actual signal.[8]

Field emission If a PMT is operated at an excessive voltage, electrons may be emitted from the dynodes by the strong electric field, causing the dark current to increase abruptly.[8]

Scintillation from glass caused by environmental sources When muons, one of many types of cosmic rays, pass through the glass envelope, Cherenkov radiation may occur, releasing a large number of photons. In addition, most glasses contain a tiny amount of the radioactive isotope ^{40}K which emits beta and gamma rays which may cause additional pulses. Furthermore, environmental gamma rays emitted from radioisotopes contained in buildings can be another source of unwanted PMT pulses.[8]

The radioactive decays and scintillation in the PMT glass leads to so-called correlated dark rate events, compared to the thermionic dark rate events which are called uncorrelated dark rate.

2 Experimental setup

For the measurements in this thesis, the PMT model R15458 by Hamamatsu was used. It is a 3-inch PMT with high gain adapted for the use in the IceCube mDOM. Compared to the conventional 10-inch hemispherical photomultiplier tubes, the R15458 is much smaller in order to fit 24 of them in one pressure vessel.[9] With these small PMTs, the pressure vessel could be small enough to fit in the boreholes which have limited size due to drill power consumption restrictions.

For the room temperature and threshold measurements, a copper dark box was used to shield the PMT from ambient light. For low temperature measurements, a smaller dark box was used which fits into a climate chamber (TestEquity 1000 series, model 1007c, with a temperature range from −73 °C to 175 °C[10]).

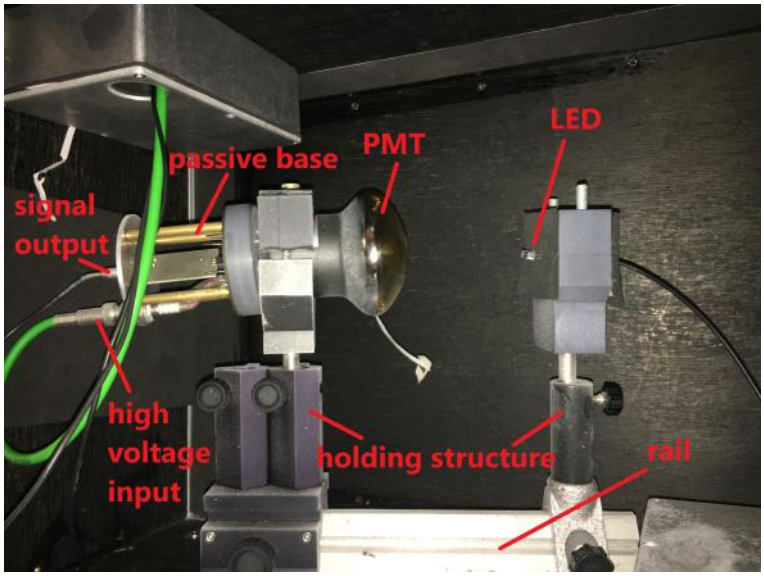

Figure 2.1: *Setup inside the dark box and the temperature chamber: On the left side of the picture is the passive base attached to the high voltage (green cable) and the signal cable (black cable). The passive base is also attached to the PMT, which is held by the holding structure on the rail. On the right side of the picture, a LED used as light source is mounted onto another holding structure.*

In both cases, room and low temperature measurements, the PMT is placed inside the box on a rail and holding structure (figure 2.1). To attach it to the high voltage and to get a signal, the passive base is needed, which is attached to the photomultiplier tube (figure 2.2). The high voltage is supplied by a C.A.E.N. model SY 403 64 channel high voltage system. To measure signals a LeCroy waverunner 6100 oscilloscope was used.

Figure 2.2: *PMT (left side) with passive base (right side).*

For light measurements at room temperature, a PicoQuant PDL 800-B laser driver and a Rigol LXI DG1022 two channel function generator were also used. The purpose of the function generator is to control the laser and to trigger the oscilloscope when a signal pulse caused by a photon from the laser is expected. For the low temperature measurements a blue LED was used. The LED is operated at a voltage between 3.35 V to 3.72 V, to get enough light at low temperatures. In both cases the light source is pointed towards the centre of the photocathode in order to reduce scattering.

The oscilloscope measures two different kinds of waveforms, shown in figure 2.3. One waveform has no signal (orange waveform in figure 2.3), meaning no photon was detected. It is constant on the same level around zero, which is the noise of the oscilloscope. This type is called baseline. The other kind of waveform has a peak (blue waveform in figure 2.3), which reaches below the noise level. This occurs when the PMT detects a photon.

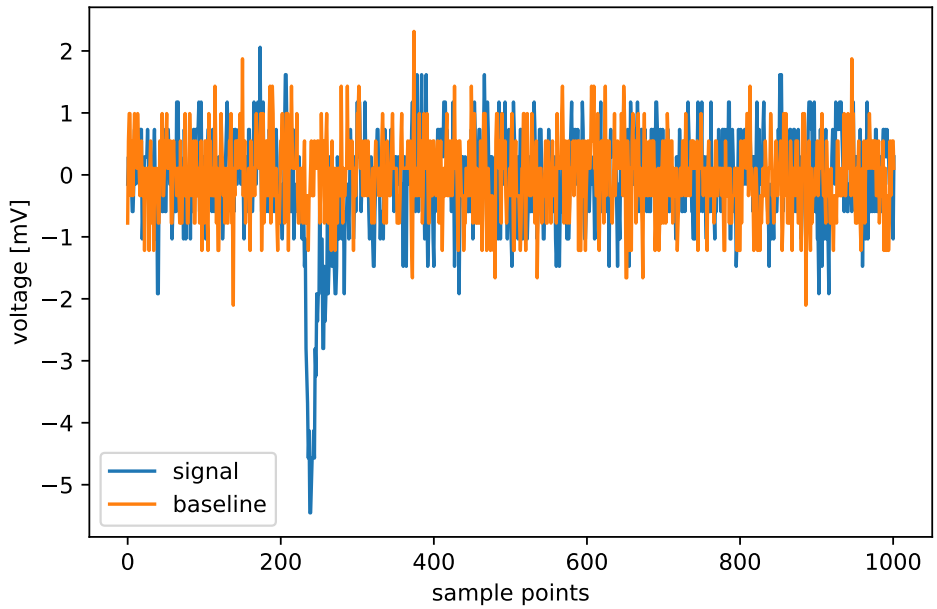

Figure 2.3: *Two kinds of photomultiplier signals: baseline (orange) and signal (blue).*

The horizontal interval of the oscilloscope, that means the time step between two samples, is variable, in case of figure 2.3, it is 0.2 ns. In this thesis, most of the time, the timebase of the oscilloscope is set to either 20 ns (method 3) or 100 µs (method 1 and method 2) per division on the oscilloscope screen, which can display ten divisions. This leads, with the best possible resolution of the oscilloscope (horizontal interval of 200 ps for 20 ns/div and 1 ns for 100 µs/div), to 1 000 002 sample points per waveform and a length of 1.000 002 ms in case of 100 µs/div.

3 Explanation of the different measurement methods

There are different ways to measure the dark rate. In this thesis three different approaches were used. The first procedure is mainly used in Erlangen, the seceond approach is mainly used in Münster and the third has been used before by various groups, but was not used until now for the latest design configuration of the mDOM PMT. These methods will be described in the following sections.

3.1 Method 1

For the first measurement method, the oscilloscope measures the time between a certain number of negative PMT signals that fall under a certain voltage threshold. This is done with a holdoff function of the oscilloscope.

Holdoff can be expressed either as a period of time or an event count. For this method the holdoff by event is used. Holdoff disables the trigger circuit for a given number of events after the last trigger occurred (in case of method 1, the number of events is $n = 100$). Events are the number of occasions on which the trigger condition is met after the last trigger. The trigger will again occur when the holdoff has elapsed and the trigger's other conditions are met.[11]

For this method, the oscilloscope parameter Dtrig time is measured. Dtrig time can be described as the time from the previous trigger to this trigger.[11] This is the mean time Δt in the equations 3.1 and 3.2 below.

To get enough statistics, the above described method is repeated $N = 100$ times.

The mean time Δt (mean over N=100 repeated measurements) between trigger events gives the rate r:

$$r = \frac{n}{\Delta t}. \tag{3.1}$$

The rate error Δr can be measured with the following equation:

$$\Delta r = \frac{n}{\Delta t^2} \cdot \frac{\sigma(\Delta t)}{\sqrt{N}}, \tag{3.2}$$

where $\sigma(\Delta t)$ is the standard deviation of the $N = 100$ measured mean times.

This method was designed to take both the correlated and the uncorrelated dark rate events into account and measure them. So method 1 should measure the total dark rate.

3.2 Method 2

For the second measurement method, data is created by recording oscilloscope waveforms with the computer. This is done by saving the data of channel 1 of the oscilloscope, where the PMT signal is the input. The idea is to trigger the signal randomly by the noise of channel 2 and transfer the voltage values of this randomly triggered PMT waveform as an array to the computer. The length of such a waveform is 1 ms, as mentioned in chapter 2.

Then a computer algorithm using the scipy.signal.find_peaks function from python counts the signals under a certain voltage threshold.

To get enough statistic, 1000 waveforms are recorded. The total time interval of all waveforms combined is 1 s. The typical number of counted peaks in 1000 waveforms is of the order of 100.

The rate r is determined with the formula:

$$r = \frac{c}{t}, \tag{3.3}$$

where c is the total number of counts and t the total amount of time. The rate error Δr can be calculated with the following equation:

$$\Delta r = \frac{1}{t} \cdot \sqrt{c}. \tag{3.4}$$

Method 2 was created to measure both correlated and uncorrelated dark rate events. Therefore it should produce the total dark rate as result.

3.3 Method 3

The third measurement method measures time differences between signals similar to method 1, but there is no holdoff. That means the time difference between each signal is measured. The distribution of the time differences is recorded with the computer. Two examples of this distribution are shown in figure 3.1 and 3.2.

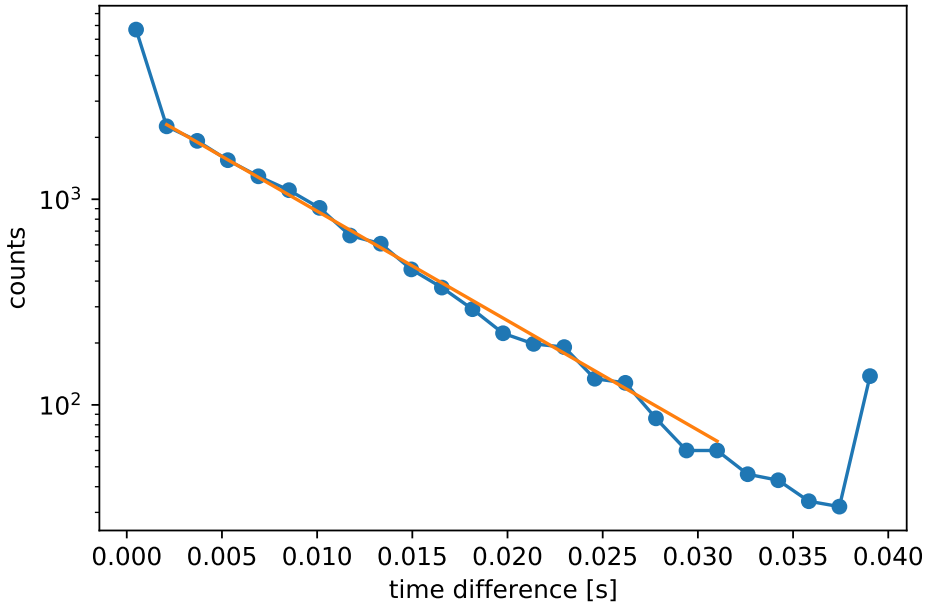

Figure 3.1: *Logarithmic count distribution of time differences (blue dots) between each signal with exponential fit (orange line) to get the rate. Measurement at room temperature with small time differences.*

Since the dark rate is Poisson distributed, the time differences δt between signals follows an exponential function:

$$c(\delta t) = e^{-a\delta t} \tag{3.5}$$

$c(\delta t)$ is the number of dark rate events in a certain time difference interval δt in seconds. An exponential fit is performed and the slope of the fitted curve is a. a is the rate in Hz. The error for this method is the fit error for parameter a.

The sampling mode of the oscilloscope was used. This enables the measurement of complicated event sequences over large time intervals.[11] For the processing, the math tool Trend was utilised.

The Trend function is a waveform composed of parameter measurements arranged in the order the measurements were made.[12] In this case each value of the waveform is one time difference measurement.

The first and the last bin of the histogram in figure 3.1 are disproportionately higher, because in these bins also higher or lower time differences are stored. Smaller time differences than zero occur due to the oscilloscopes Trend Function (see figure 3.2).

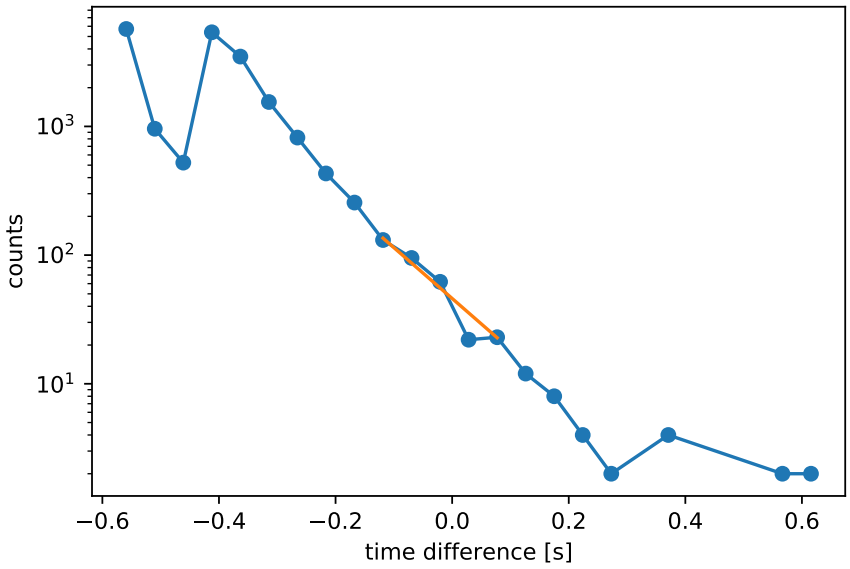

Figure 3.2: *Logarithmic count distribution of time differences (blue dots) between each signal with exponential fit (orange line) to get the rate. Measurement at* −40 °C *with large time differences.*

Histograms from other measurements, like figure 3.2, have greater discrepancy from the exponential part in the first and the last bins. Therefore, just the exponential part of the histogram was used in order to get the dark rate. This is due to the distinction between correlated and uncorrelated dark rate. The correlated dark rate occurs at smaller time differences and does not decrease exponentially and therefore is neglected in this method. That means that in comparison to the other two methods, which count both types of dark rate events, method 3 only counts uncorrelated dark rate events.

To get the slope of this exponential part, the fit limit for the lower bound was chosen by eye. The upper bound is the point at which the counts fall below a threshold of 10 to 50 counts depending on how good the upper end of the scale still fits with the exponential part.

3.4 Measurements with light source

For the measurements with a light source, a function generator was used to drive a laser or LED which illuminated the PMT with short light pulses. The oscilloscope triggered on the pulses generated by the function generator.

This technique is used to get a defined quantity of photons per pulse and thus a defined number of photoelectrons. The multiplicity of the number of photoelectrons is Poisson distributed. The response of a PMT to several of these light pulses can be modelled quite well by the so-called PMT response function (figure 3.3), which can be fitted to the resulting charge spectrum. And thus get information about the gain for example.

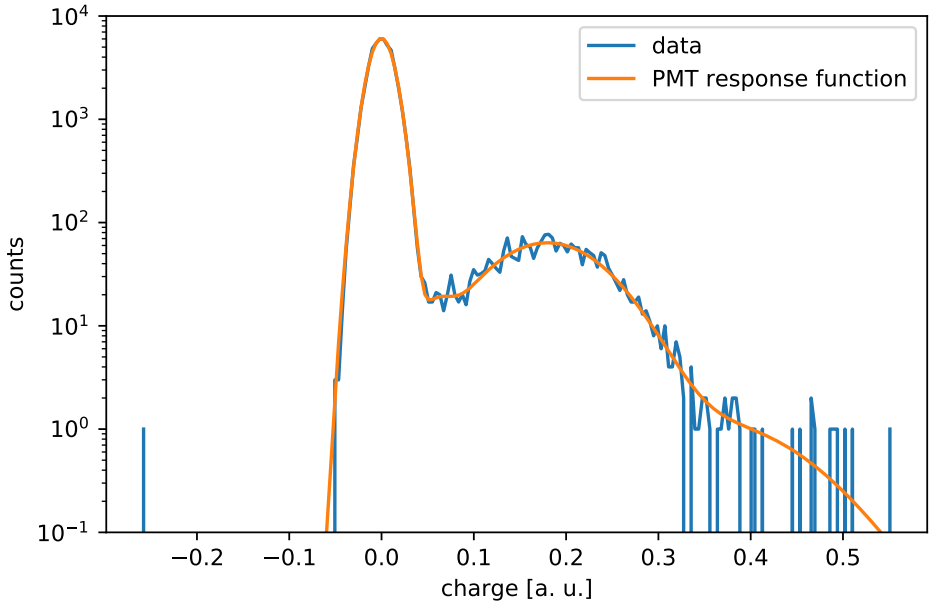

Figure 3.3: *Charge spectrum of a PMT response to light illumination with fitted PMT response function.*

Dark rate measurements are not suitable for the gain determination, because the signal multiplicity distribution is not Poissonian and changes from PMT to PMT. Therefore the PMT response function cannot be fitted as easily as with the light source measurement.

The frequency of the frequency generator is set to 1 kHz to have enough time between two triggers to not measure accidentally afterpulses from the last signal. To get a good resolution of the single photoelectron peak, one measures in the single photoelectron regime. As already mentioned in section 1.3.2, the mean number of photoelectrons per pulse has to be much lower than one. For the measurements done in this thesis, the mean number of photoelectrons is most of the time about 0.04.

Two different measurements were done with the light source: the gain measurement and a cross-check for the threshold measurement. The first application possibility was already described theoretically in section 1.3.2.

To extract the gain out of a single photoelectron spectrum the measured position of the pedestal and the single photoelectron peak from the PMT response function were used. To calculate the gain, equation 1.2 was used. To derive a charge from the measured voltage one has to calculate the current which caused the voltage drop at the internal resistance of the oscilloscope (50 Ω) via Ohm's law. This current can then be integrated over time to get the charge.

The amplitude spectrum for the threshold measurement is shown in figure 3.4. On the right side near zero is the pedestal peak and next to it on the left the single photoelectron peak. The amplitude spectrum is generated by plotting the minimum of each recorded waveform in a histogram. The use of different trigger thresholds can be emulated by using cuts on the amplitude distribution. The threshold cuts are depicted by the vertical lines in figure 3.4. Each signal in the histogram below this cut is counted and divided by the sum of all counts below the smallest threshold to get a relative number of signals. That means the relative number of signals that survive the cut can be compared to other threshold measurements.

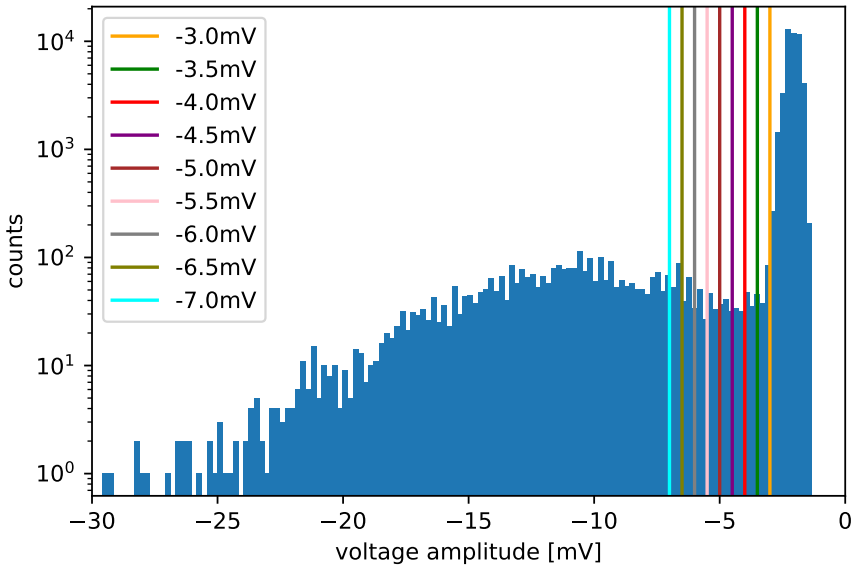

Figure 3.4: *Histogram of the Amplitude spectrum of the PMT measured with a pulsed light source. On the right side near zero is the pedestal peak and next to it on the left the single photoelectron peak. The threshold cuts are depicted by the vertical lines.*

4 Measurements

As already mentioned in chapter 2 measurements at different temperatures but also measurements with different threshold levels were performed. How they were done and what results these measurements delivered will be discussed in this chapter.

4.1 Gain Measurements

For each PMT and for each temperature, the high voltage needed to achieve a gain of 5×10^6 (nominal gain) has to be measured. This was done with the light-source measurement setup. The single photoelectron spectrum for a certain high voltage was recorded. The gain was calculated as explained in section 3.4.

Four high voltage values around the high voltage value for the nominal gain given by the manufacturer for the used PMT were measured (between 950 V and 1190 V). On a double-logarithmic scale, the gain follows the high voltage linearly and is called the gain slope. The high voltage for the nominal gain is extracted via a linear fit to the gain slope.

Measurements at the temperatures 21 °C, 10 °C, 0 °C, −10 °C, −20 °C, −30 °C and −40 °C were done. For each measurement the operating voltage for the nominal gain varies from 978 V to 1010 V, although it was always the same PMT. The high voltage rises almost linearly with the temperature. This can be seen in figure 4.1. The error in this plot is due to rounding error and has the value of 1 V.

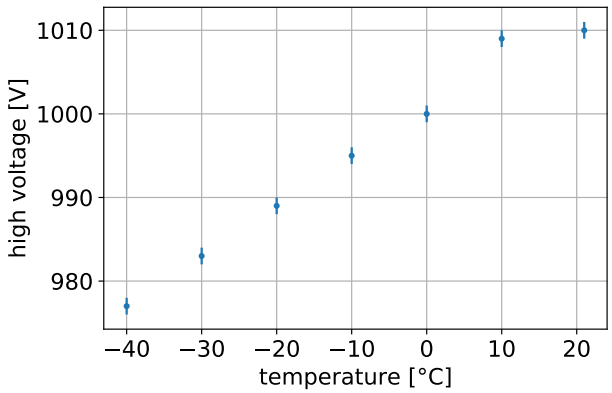

Figure 4.1: *Operating voltage as a function of temperature for the PMT used for the temperature measurements.*

The result of figure 4.1 is similar to the result of a gain-voltage-temperature characterisation in [5]. Although the voltage measured in [5] is in general higher (different PMTs have different voltage values for the same gain value), while the linear tendency is the same.

4.2 Threshold Measurements

For the threshold measurement, all three methods and the measurement with the light source were used to measure with different voltage threshold levels. One measurement cycle consists of the threshold levels: −3 mV, −3.5 mV, −4 mV, −4.5 mV, −5 mV, −5.5 mV, −6 mV, −6.5 mV and −7 mV. This cycle is measured several times to get the mean rate for the threshold level. That cycle procedure can be seen for example in figure 4.2 for method 1. The first −3 mV measurement was completed after 48 s. Then the first −3.5 mV measurement followed and so on. The second −3 mV measurement ended about 9 min after the first one. This is also the explanation for the time variation in figure 4.4 and figure 4.6. One measurement for method 2 took about 7 min, due to waveform processing time. A method 3 measurement was completed after approximately 1 min.

For method 1, the measurement of the dark rate over time is shown in figure 4.2. The dark rate was calculated using the formula 3.1 and the error in this figure is derived from equation 3.2. Each colour represents one threshold level. So the figure shows that the closer the threshold value is to the baseline, the higher the rate, because more signals surpass the threshold. This phenomenon can also be seen in figure 4.3, where the mean rates are plotted over the threshold level. Here, the mean rate ranges from

132 1/s to 208 1/s. The error Δr in figure 4.3 is given by the equation:

$$\Delta r = \frac{\sigma(r)}{\sqrt{N}} \tag{4.1}$$

were $\sigma(r)$ is the standard deviation of the mean rates and N the number of measurements.

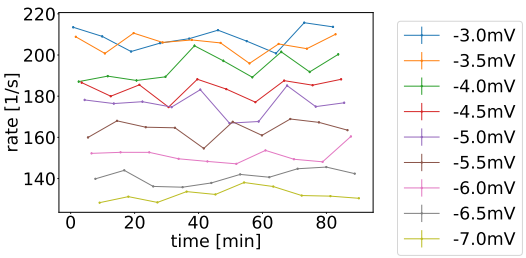

Figure 4.2: *Measured dark rate over time for threshold measurement of method 1.*

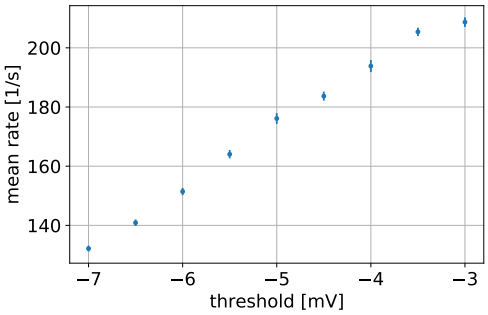

Figure 4.3: *Mean dark rate versus threshold value for method 1.*

For method 2, the measurement of the dark rate over time is shown in figure 4.4. The dark rate was calculated using the formula 3.3 and the error in this figure is derived from equation 3.4. Again each colour represents one threshold level. The difference between each threshold level is not that clear, because for this method, the rate variation is very big. But also a decrease in the mean rate can be seen in figure 4.5. Here, the mean rate ranges from 137 1/s to 234 1/s. The mean rates of this method are in general higher than for method 1. The error in figure 4.5 is given by equation 4.1.

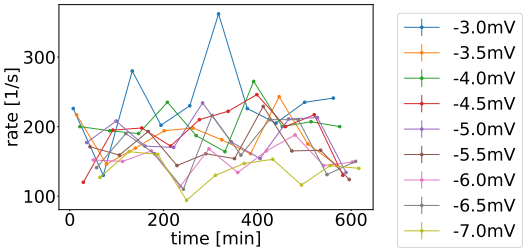

Figure 4.4: *Measured dark rate over time for threshold measurement of method 2.*

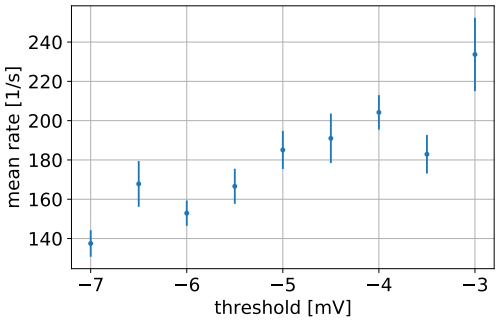

Figure 4.5: *Mean dark rate versus threshold value for method 2.*

For method 3, the measurement of the dark rate over time is shown in figure 4.6. The dark rate was calculated using formula 3.5 and the error in this figure is derived from the fit error for parameter a of equation 3.5. Again each colour represents one threshold level. Here, the rate increases for all threshold levels over time. This might be due to changes in temperature in the chamber or something else that was not recorded or monitored. The mean rates in figure 4.7 are still meaningful, because the rate values (shown in figure 4.6) increase for all thresholds approximately evenly. Here, the mean rate ranges from 87 1/s to 129 1/s, which is lower than for method 1 and method 2, because only the uncorrelated dark rate is measured. The error in this mean rate plot is given by equation 4.1.

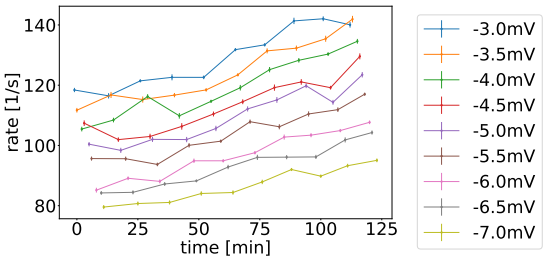

Figure 4.6: *Measured dark rate over time for threshold measurement of method 3.*

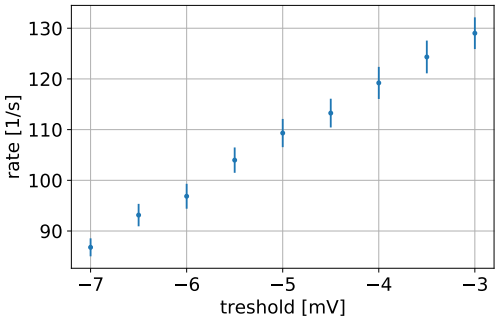

Figure 4.7: *Mean dark rate versus threshold value for method 3.*

This type of measurement was done with three different PMTs, which show equal results. All threshold measurements presented here were done with the PMT with the serial number BA0796. An Amplitude spectrum measurement with a light source was performed in addition for the PMT BA0796. This measurement method is explained in section 3.4.

All the mean rates of these measurements are shown in figure 4.8. To achieve better comparison, the mean rates are divided by the mean rate for -3 mV of the corresponding method. So the relative decrease in mean rate is displayed in figure 4.8.

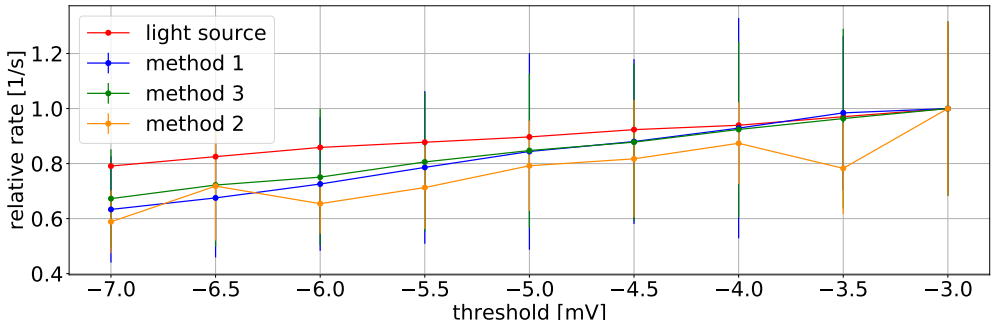

Figure 4.8: *Mean rate ratio for all measuring methods for the BA0796 PMT.*

For all methods, the relative rate decreases when the threshold gets lower. The three measurement methods' slopes look similar, but the curve measured with the amplitude spectrum is different. This might be due to the difference in the multiplicity distribution, meaning the difference in single photoelectron or two photoelectron events in the light source measurement and dark rate events.

4.3 Temperature Measurements

The temperature measurements were performed to get information about the dark rate behaviour at low temperatures. To monitor the dark rate over time and to gain more statistics, long term measurements of 12 to 20 hours were used for the temperature measurements. A long term measurement consists of 72 repetitions of consecutive measurements of all three methods. With decreasing temperature, the measurement took longer, because the amount of dark rate events decreases, but a certain amount of events was needed to calculate the dark rate. Especially for method 1 the measurement time increased.

The threshold level for the temperature measurements is $-3.5\,\mathrm{mV}$. This level was used, because at this voltage, many signals are counted, but it is still above the noise level of the oscilloscope. So we assume that only a small amount of signals that contribute to the dark rate get lost and no noise is wrongly added to the signals.

Examples for such long term measurements comparing the three methods in a plot are shown in figure 4.9, figure 4.10 and figure 4.11 for different PMTs each.

The measurement in figure 4.9 shows the result of a room temperature long term measurement shortly after exposure to room light. Here, the exponential decrease, already mentioned in section 1.3.4, can be seen. In this case, it takes about three to four hours to get to a constant dark rate level. Like in the threshold measurement, also

here method 2 has a great variance in its dark rate values. For this measurement the difference between method 1 and method 2 are not that severe than in measurements with other PMTs or lower temperature, which can be seen later. The mismatch between those two methods and method 3 is as expected, due to the lack of correlated events in method 3.

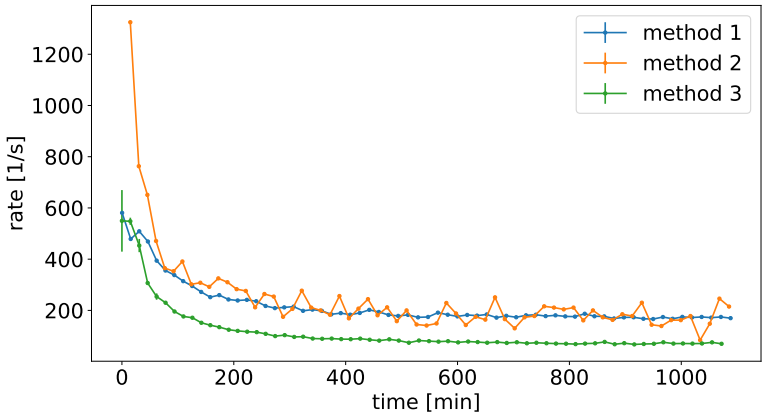

Figure 4.9: *Long term measurement with PMT BA0805 shortly after exposure to room light at room temperature for the three different measurement methods. In all three measurement methods, an exponential decrease in rate can be seen over time.*

For low temperature measurements (figure 4.10), the variance in method 2 became even larger, and the values were not on an equal level as for method 1, although a similar level was expected. Both method 1 and 2 should measure correlated and uncorrelated dark rate events and therefore should have similar values, but they deliver very different results (shown in table 4.1). Why this is the case will be explained in chapter 5. For each low temperature measurement the development of method 2 looks different.

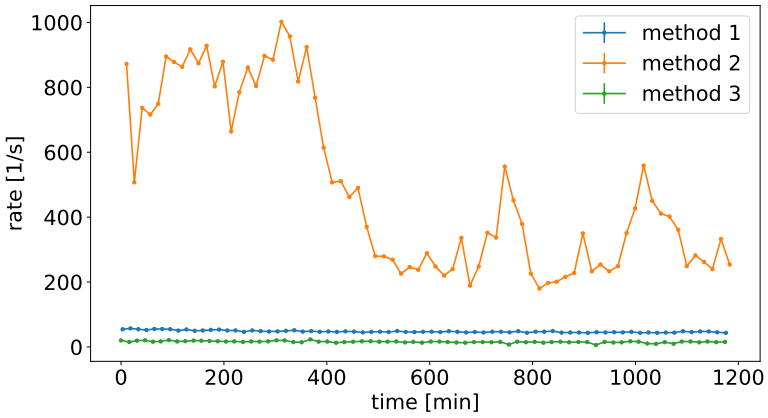

Figure 4.10: *Long term measurement with PMT BA0721 at −30 °C for the three different measurement methods.*

At one point, a spike in the rate (figure 4.11) can be spotted. This might be due to electronic noise which originates from other devices, possibly even from the climate chamber. This noise most likely couples into the oscilloscope signal through the power supply. If many of those oscillating signals occur after each other in a small time window, the oscilloscope triggers and counts those oscillations as dark rate events. The spike event was filtered and does not appear in the data.

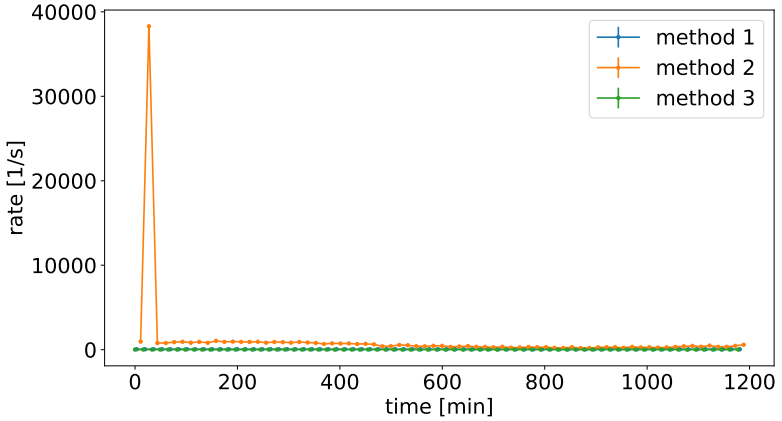

Figure 4.11: *Long term measurement with PMT BA0721 at −20 °C for the three different measurement methods. In method 2 a spike can be seen.*

Longterm temperature measurements were done at 21 °C, 10 °C, 0 °C, −10 °C, −20 °C, −30 °C and −40 °C with PMT BA0721. For the 21 °C measurement, the climate chamber was not running, so the temperature variation might be a bit higher than for the other measurements where the temperature was controlled.

From these longterm temperature measurements, the mean rate was calculated and was plotted against the temperature. The results are shown in figure 4.12. Note that the left y-axis is valid for method 1 and method 3 and correlated (explained later). The right y-axis displays the mean rate values for method 2. This action was needed, because method 2 has much higher values than method 1 and method 3 due to the generally higher dark rate.

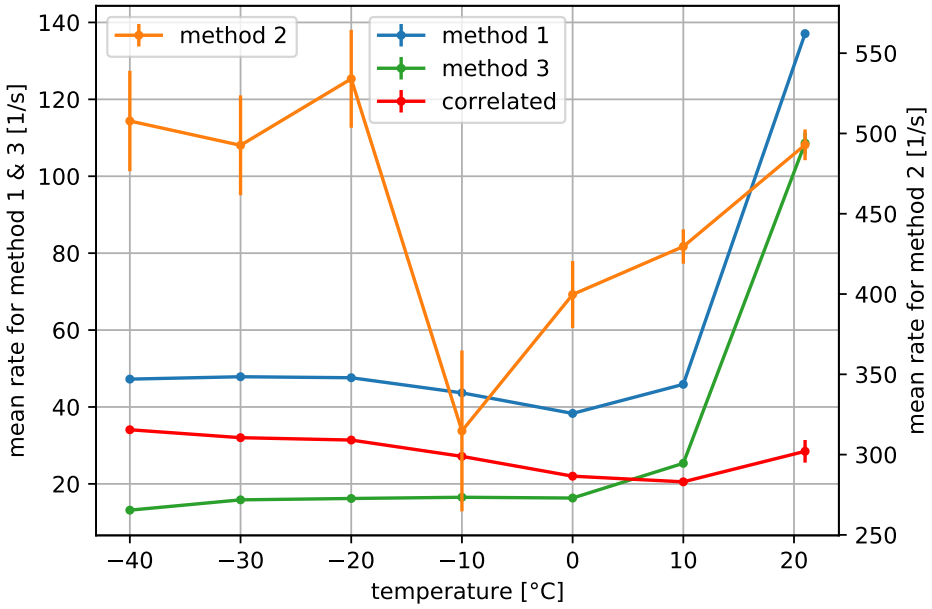

Figure 4.12: *Mean rates of temperature measurements versus temperature. The correlated data set contains the difference of method 1 and method 3 (correlated dark rate). The left y-axis is valid for method 1 and method 3 and the calculation of the correlated dark rate. The right y-axis displays the mean rate values for method 2.*

Method 1 and method 3 show the behaviour that was expected. With falling temperature, the fraction of thermionic emission decreases and the mean rate drops. Below 0 °C the mean rate for method 1 rises slightly, due to the correlated event contribution. These correlated events were plotted individually to show the rising tendency of method 1 with lower temperatures. This phenomenon can be explained with a rising amount of scintillation. The correlated dark rate was derived by subtracting the mean dark

rate of method 3 from the mean dark rate of method 1. That dark rate behaviour was also observed by [5]. Method 1 yields a higher rate than method 3, because it also contains the correlated background events. In table 4.1 this can also be seen. The difference between method 1 and method 3 ranges from approximately 20 1/s to 34 1/s (see table 4.1 column Correlated).

Temperature	Method 1 [1/s]	Method 2 [1/s]	Method 3 [1/s]	Correlated [1/s]
21 °C	137.1 ± 0.98	493 ± 9.59	108.6 ± 2.77	28.5 ± 2.94
10 °C	45.9 ± 0.16	430 ± 10.71	25.4 ± 0.56	20.5 ± 0.58
0 °C	38.3 ± 0.25	400 ± 20.83	16.3 ± 0.28	22.0 ± 0.37
−10 °C	43.7 ± 0.21	315 ± 50.08	16.5 ± 0.24	27.2 ± 0.32
−20 °C	47.6 ± 0.25	534 ± 30.49	16.2 ± 0.31	31.4 ± 0.40
−30 °C	47.9 ± 0.39	493 ± 31.08	15.9 ± 0.33	32.0 ± 0.51
−40 °C	47.2 ± 0.26	508 ± 31.26	13.2 ± 0.30	34.1 ± 0.40

Table 4.1: *Numerical values for the mean rates of the temperature measurements. The correlated data set contains the difference of method 1 and method 3.*

5 Analysis and Comparison of the methods

All three methods deliver slightly different results. This is because method 1 and method 2 count besides the typical dark rate events also the correlated background events. These events are excluded in method 3.

Method 1 can be used to gain knowledge about the total dark rate. Due to measuring the time between a certain number of events, it can distinguish, just up to a certain point, between events that follow shortly after each other, and might therefore be correlated.

This procedure seemed to work very good in this thesis. The different threshold levels were very distinguishable, and the temperature measurements delivered results that were comparable to other measurements performed by different groups with different setups.

The analysis of the data was easy for this method. There were no problems concerning the collection or processing of the data.

Method 2 should deliver results that include all parts of the dark rate, correlated and uncorrelated events. It is doing so by counting all events occurring within 1 s.

This approach did not work as expected. The variance of the measured dark rate values was very high. For the threshold measurements, no very clear distinction between different threshold levels could be made. The temperature measurement results are not even close to the results of the other two methods.

The problem with this method is that the oscilloscope is not able to process every waveform correctly. It saves some waveforms multiple times instead of saving a new one. This happens for waveforms with peaks in it about 67% of the time. The reason, why these repeated waveforms could not be sorted out to get every waveform just once, is that they do not get repeated the same amount of times. Sometimes, the oscilloscope gets different waveforms after each other, as it should, and the waveform does not get repeated at all. Therefore, it is impossible to figure out how many of the

waveforms containing no peaks are wrongly saved. The technical reason for this faulty behaviour of the oscilloscope could not be determined in this thesis.

By counting the peaks of some of the waveforms multiple times, the dark rate is distorted. This might be the reason for the high dark rate value fluctuations for this method, which could be seen in chapter 4.

The analysis of the data this procedure delivered was not very error prone. A more sophisticated algorithm, to detect recurring waveforms has to be developed for future measurements.

Method 3 delivers the opportunity to only measure the uncorrelated dark rate events. This is achieved by measuring the slope of the linear part of the logarithmic histogram of time differences between signals. Therefore this method is not that well comparable to the other two methods, but allows to distinguish between the correlated and uncorrelated dark rate by comparison with method 1.

This procedure seemed also to work very well in this thesis. The different threshold levels were distinguishable, and the temperature measurements delivered similar results as other temperature measurements that were already performed by different groups with different setups.

The analysis of the data for this approach was a bit difficult, because the fit procedure had to work for each of the 72 data sets in the measurement. In some cases the whole exponential part was taken into account for the fit and in some cases just three points were in the fit range. This was the case due to a wide range of time differences measured in different data sets. For some data sets at room temperature the largest time difference is about 0.04 s (figure 3.1), and for the −40 °C measurement time differences of approximately 1.2 s (figure 3.2) are possible. But it was not necessary to fit each data set individually, because the slope was represented well enough by the parameter settings for the fit that suited every data set.

Comparison of the methods results is almost impossible, because method 1 and method 2 do not measure the same as method 3. The two methods that should deliver similar results are not comparable, because method 2 had technical issues. Nevertheless method 3 supports the results of method 1. The reason is that both methods have similar curve developments for the temperature measurements. It can be also seen that the dark rate values, shown in table 4.1, are not very far apart. The discrepancy of this two methods can be explained with the different types of dark rate they measure.

6 Conclusion

The aim of this thesis was to compare different procedures to measure the dark rate for photomultiplier tubes, used for the IceCube mDOM, with an oscilloscope.

Method 1 measured the time between a certain number of PMT signals that fall under a certain voltage threshold. Method 2 counted with a computer algorithm the amount of peaks in prerecorded waveforms. Method 3 measured the time difference between every signal. Additionally measurements with light source were performed to get information about the gain and to cross-check the threshold measurement.

The gain measurement at different temperatures demonstrates that the nominal high voltage decreases with decreasing temperature. The performed threshold measurement shows that with lower thresholds less events get counted and that 0.5 mV step levels are very distinct and all methods decrease almost in the same manner, except the light source method. The temperature measurement displays that the dark rate decreases with lower temperature until a certain level is reached and then increases slightly.

Summarising the methods results, it can be said that method 1 and method 3 can be used right away to calculate the total and uncorrelated dark rate for PMTs, respectively. The general idea of method 2 should be also fine, but the practical implementation should be improved.

The next step would be to solve the technical problems for method 2 in order to have access to another working dark rate measurement method for further comparisons.

Bibliography

[1] ECAP. *IceCube*. URL: https://ecap.nat.fau.de/index.php/research/neutrino-astronomy/icecube/. (accessed: 04.03.2021).

[2] M. G. Aartsen et al. *Neutrino astronomy with the next generation IceCube Neutrino Observatory*. 2019. arXiv: 1911.02561 [astro-ph.HE].

[3] *Birds Eye Upgrade Geometry*. URL: https://www.sense-pro.org/images/Portraits/institutes/IC/Birds_Eye_Upgrade_Geometry.jpg.

[4] Lew Classen. 'The mDOM – a multi-PMT digital optical module for the IceCube-Gen2 neutrino telescope'. PhD thesis. Friedrich-Alexander-Universität Erlangen-Nürnberg, 2017.

[5] D. van Eijk, J. Schneider and M. Unland. *Characterization of Two PMT Models for the IceCube Upgrade mDOM*. 2019. arXiv: 1908.08446 [astro-ph.IM].

[6] *mDOM Picture*. URL: https://www.uni-muenster.de/imperia/md/images/physik_kp/agkappes/icecube/fittosize_341_395_8b231979e37ed23a4f77%200fba923f64ec_mdom_midres.jpeg.

[7] Claus Grupen. 'Teilchendetektoren'. In: first edition. BI-Wiss.-Verl., 1993. Chap. 5.1 Photomultiplier, pp. 205–213. ISBN: ISBN 3-411-16571-5.

[8] Hamamatsu Photonics K.K. *Photomultiplier Tubes. Basics and Applications*. fourth edition. Hamamatsu Photonics K.K., 2017. URL: https://mf2ap081.marsflag.com/hamamatsu__jp_en__jp_en/clf.x?c=1614874619270&mode=__ALL__&s=PjovQkkIsn4Bo9Z-q69FVwJgwGkjlGGMB3OGWVJKF6PjYXOvuDPimDx%20kGFR-bQypO2zc1pg1NWhrDndL922SOEzstRzV65UBn4_jZwSu2gzJowSEPgggX3G%20qdJkzuFKw6GogYMnTTAqpqKtXd1tJ6yk7JeP5MBUDKAJLRGDFGvhdqth6A3l4_r-AJY_KHpgMxONaReNBev4.&v=1614874510990.

[9] Hamamatsu Photonics K.K. *Photonic Devices 2020*. Hamamatsu Photonics K.K. URL: https://mf2ap081.marsflag.com/hamamatsu__jp_en__jp_en/clf.x?c=1615281345673&mode=__ALL__&s=Xt6EWnAG346tlDtum9RvMrfYCrKplQdgi4J%20z95RJcR7ms6WjSa_uhcfH9LF4moDB2vLELQrlnaYI9792r_Yz7Lp5XdhSpx-I_xltSRNGfzfS41OgNqox9ourecJbO5ufUvI_DBMtyHeDfBcHrUGLp9HY8TwSytERWkqdfs-f47MiyRJINBhdrb7xDodJSXLArl-t2rHjC_o.&v=1615281328771.

[10] TestEquity LLC. *TestEquity 1007C Temperature Chamber (Environmental Chamber)*. URL: https://www.testequity.com/product/13039-1-1007C. (accessed: 09.03.2021).

[11] LeCroy Corporation. *WaveRunner 6000A Series Operator's Manual*. LeCroy Corporation, 2007.

[12] LeCroy Corporation. *Appliction brief. Trends, Tracks, and Histograms (LAB:WM769)*. LeCroy Corporation.

Acknowledgements

I want to give many thanks to Jonas Reubelt for the provision of the interesting thesis topic, the great supervision and the programming teaching. Also I want to thank the Erlangen IceCube working group for the friendly and welcoming atmosphere, the insight in the huge IceCube project and the support writing my thesis.

Thanks go also to my friends and family, helping me through frustrating times, when the oscilloscope did unexpected things again.

Eigenständigkeitserklärung

Hiermit versichere ich, dass ich die vorliegende Bachelorarbeit selbstständig verfasst habe. Ich versichere, dass ich keine anderen als die angegebenen Quellen benutzt und alle wörtlich oder sinngemäß aus anderen Werken übernommenen Aussagen als solche gekennzeichnet habe, und dass die eingereichte Arbeit weder vollständig noch in wesentlichen Teilen Gegenstand eines anderen Prüfungsverfahren gewesen ist.

Erlangen, den 04.05.2021 **Anna Eimer**